

Downlink channel analysis at multi-cell massive MIMO: novel adaptive channel allocation scheme

Sandeep Dhanraj Bawage, Manjula Shivkumar

Department of Electronics and Communication Engineering, Lingaraj Appa Engineering College, Bidar, Karnataka, India

Article Info

Article history:

Received Dec 8, 2021

Revised Apr 4, 2022

Accepted May 8, 2022

Keywords:

Channel allocation

Downlink

Multi-in-multi-out

Throughput

Wireless communication

ABSTRACT

In large multiple-input multiple-output (MIMO) systems, we offer a new access strategy for crowd situations. Crowd situations include a high number users who have intermittent access patterns, making orthogonal scheduling impossible. In this paper, the work is driven by the massive MIMO problem at crowded environment. The pilot contamination problem is dependent on the protocol assumptions is observed in the system. We investigate a crowd situation in which the users number and their access behaviours make scheduling broadcasts impossible. The pilot assignment is time-slot randomized, but the data portion is repeated, allowing it to use successive-interference-cancellation across copies of comparable packets. In result analysis, the transmission of downlink to the user has shown with changing the number of users, fading effect, transmission power and the number of base station antennas.

This is an open access article under the [CC BY-SA](#) license.



Corresponding Author:

Sandeep Dhanraj Bawage

Department of Electronics and Communication Engineering, Lingaraj Appa Engineering College

Bidar, Karnataka, India

Email: sandeepbawage@gmail.com

1. INTRODUCTION

Recently, MIMO has been assumed one of the most important technologies for fifth generation (5G) and sixth generation (6G) wireless communications [1], since it can fulfil the needs for higher spectral efficiency (SE), energy-efficiency (EE) and coverage probability [2]. Moreover, Massive-MIMO allows a BS to serve several numbers of user-equipment (UE) with the resources of time-frequency in order to improvise the overall performance of the system. Depending on the antenna setup, massive-MIMO can be characterized into two architectures, such as co-located and distributed massive-MIMO. Later, one finds service antennas in the compact area; the previous one spreads antennas all over the larger area. Although co-located architecture is very attractive because of lower backhaul needs, the distributed one provides high coverage probability at maximum infrastructure costs.

A massive-MIMO network has been represented in [3]; it is a form of distributed-massive MIMO. It is considered the promising network architectures for 5G wireless network based on its capability to provide coverage probability and huger throughput to all of the users throughout the system. This type of architecture spreads a tremendous number of randomly located access points (APs) over the larger network area in order to serve a smaller number of single UEs antennas as an alternative to the small network cell. In order to have interference management and efficient resources among more than one APs, an unspecified backhaul link joins all the APs to the central processing unit (CPU) [4]. The utilization of antennas at BS makes the training process massive-MIMO in downlink prohibitively [5]. It is common to consider time-division duplexed (TDD) process with the help of uplink training, resulting in minimized CSI-acquisition times. Anyways, while working in TDD, system is considered to work inside the perfect channel assumption [6]. Anyways, the receive and

transmit radio-frequency (RF) chains at UEs and BS are not calibrated [7], violating the assumption of channel reciprocity.

The massive-MIMO can broadly be categorized into two classes: performance analysis in errors of reciprocity calibration [8] and methods for reciprocity calibration [9]. While these methods give accurate calibration between downlink and uplink RF chains and errors of residual calibration, exist that can limit the performance system. It becomes necessary to examine the massive-MIMO system performance in reciprocity calibration errors. The effects of reciprocity-calibration errors have been studied as multiplicative [10] and additive [11] errors in coefficient channels at BS. The model of multiplicative error is preferable because of its capability to catch the RF mismatches. In order to achieve the effects of multiplicative reciprocity on the signal-to-noise-ratios (SINRs) of the massive-MIMO system in linear-precoding methods have been assumed in [12]. According to Bjornson *et al.* [13] the reciprocity errors are introduced as uniformly distributed as well as random variables in [14]; they can be modelled as Gaussian random variables. This method has little empirical evidence from available outcomes in [15]. According to Mi *et al.* [16] represent reciprocity imperfections that lead to achievable SINRs for the system using linear precoding. Anyways, the state-of-the-art method on modelling the effects of reciprocity imperfections in massive-MIMO explicitly considers the effective downlink-channel are perfectly known at UE that is normally not the case unless extra resources are maximized on the downlink pilots.

In order to attain the massive-MIMO benefits, each BS requires an accurate estimation of CSI either through channel reciprocity or feedback methods. In TDD and frequency-division-duplex (FDD) has been assumed. TDD is assumed to be a better mode to obtain the CSI in advanced wireless systems over the FDD due to TDD that needs estimation in one direction and utilized in both directions, while the FDD needs feedback and estimation for both reverse and forward directions, respectively. METIS and TDD have been considered for massive-MIMO [17] due to the radio resources efficient usage. Bazzi and Xu [18] introduced the utilization of FDD and possibility of utilizing FDD method methods will continue to attract more attention due to FDD, which is very common of system massive-MIMO. To examine the bases and main effects of the pilot-contamination in the system of massive-MIMO in TDD method in reducing the pilot-contamination in multi-cell systems from last decades. In the architecture of TDD, the utilization of training signals (pilot) and channel reciprocity in UL are the main key features for its application. Utilizing the reciprocity notion, it is considered the forward channel, which is similar to the reverse channel for theoretical purposes. Hence, the required channel information is achieved from the transmitted pilots on reverse link from the UTs. However, the antenna calibration method is implemented at the receiver side and transmitter side owing to various transmit or receiver RF chains [19].

The number of channel symbols for CSI estimation is assumed in [20]. In [20], number of UL pilot symbols similar to number of UTs was introduced, while in [21], it was represented that number of training symbols that is ideal may be more than the number of antennas if data power and training are needed to be similar. Most of the studies are carried out on the pilot contamination; it is considered that the similar size of the pilot signals is utilized in cells. Research by Nie and Zhao [22] have shown that in a multi-cell system, arbitrary pilot allocation is achievable of multi-cell. In wireless communication, spectral efficiency needs appropriate pilot reuse and frequency time in order to improvise the system throughput. The frequency reuse has been represented to give more efficient utilization of limited available spectrum; it is also considered unavoidable co-channel interference. In the massive-MIMO TDD-system, pilot signals are utilized to evaluate if the channel is contaminated as an outcome of non-orthogonal pilot signals in the multi-cell system of multi-cell. This phenomenon causes interference at inter-cell and is proportional to the number of BS antennas that in turn minimizes the achievable rates in spectrum efficiency and network.

The downlink in a huge MIMO system is investigated. To consume the electricity with the aid of an antenna, which is a very little amount. Under ideal conditions, each antenna uses inversely proportionate amounts of transmitted power, which is inversely proportional to the amount of antennas; under ideal conditions of transmitting SNR, the total transmission power is inversely proportional to the amount of antennas. The number of antennas, on the other hand, is inversely proportionate to the transmitting power. As a result, the amount of power used in huge MIMO applications is significantly reduced. In order to increase the number of Antennas at the BS in a massive-MIMO system, spatial resolution is improved.

The previous paper's technique uses a procedure of coded random access, the terminals transmit with a predetermined likelihood and send a pilot followed by the data portion in the uplink. The pilot assignment is randomised in each time-slot, but the data portion is repeated, allowing for SIC over several duplicates of the same packet. The suggested implementation of SIC is an application of massive MIMO qualities, since it relies on features. These features enable signal processing, which converts polluted signals into linear data combinations. Because SIC is not accessible in framed slotted ALOHA, the endpoints work similarly to the proposed method, but the likelihood of transmission is optimised for contamination-free transmissions. The drawback is rate loss, which is caused by the channel coding.

This paper shows improvised adaptive channel allocation (ACA). The proposed SIC implementation has new massive-MIMO belongings as it bank on two characteristics to this framework, such as asymptotic power invariance received from user over the user channels' time-interval and asymptotic orthogonality. These features enable the received signal processing that turns into contaminated signals as linear data combinations. These linear groupings from the codeword can be deciphered utilizing SIC to provide decontaminate signals via SIC to maximize throughput that is compared to the conventional methods. However, the SIC gain more than compensates for the rate loss caused by the channel code, resulting in much better uplink throughput than uncoded operation.

2. PROPOSED METHODOLOGY

Here, we introduce the metrics, scalars and vectors. The scripts indicate transpose and superscript simplify as conjugate-transpose, and superscript * simplifies as the complex conjugate. We consider the system of random access that contains one BS with the users and each antenna at BS with one antenna and communication is performed by using slotted-time. Whereas every time slot consists of a stage of the uplink channel; a downlink data stage is introduced in this paper. In Figure 1 represents one antenna with massive-MIMO that consists of antenna arrays, BS, and the user terminals. The BS transmits the data from different antennas into various terminals at the same frequency.

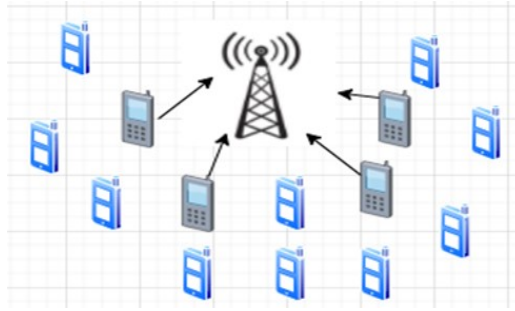


Figure 1. Single antenna with massive-MIMO

The improvised technique is introduced for qualifying the channel-allocation (CA) to resolve channel issues. In individually time-slot, every user is active with P_x probability. There are Z orthogonal channel-sequences $\{C\}$ and each sequence Z consists of the symbols $C=[c(1), c(2), \dots, c(Z)]$. An active user chooses the channel-sequence via channel-sequence from Z channel sequence. Multi users may select the equal channel-sequence. The random channel schedule with Z and U . The channel among u th user and BS at b th time-slot is simplified as $h_{b,u} = [h_{b,u}(1) h_{b,u}(2) \dots h_{b,u}(A)]^Z$ where $h_{b,u} \forall b,u$ are an i.i.d. Then, we assume the structures that applied an ideal power-control, which $h_{b,u}(m) \sim CB(0,1), \forall m$. The time-slot has Z_b that corresponds to coherence time in channel-coefficient remains const. In time-slot b , X_b denote active users, while X_b^n denotes set of the users that have chosen c_b in b 'th time-slot. If $E_j^{pk} \in C_b^{A \times Z}$ denotes uplink channel signal received in b time-slot.

$$E_j^{pk} = \sum_{b=1}^A \sum_{u \in X_b^n} h_{b,u} c_n + F_b^{pk} \quad (1)$$

where, F_b^{pk} is the matrix of Gaussian noise, hence $F_b^{pk}(m,n) \sim (0, \delta_b^2), \forall m,n$. the vector f and matrix F with various sub and superscripts follow the similar description. All the active users send the length of message M_k in the phase of uplink-data. The message from u 'th user is defined $D_u^k = [D_u^k(1) D_u^k(2) \dots D_u^k(M_u)]$. Utilizing $E_j^{pk} \in C^{A \times M_u}$ to describe the received data signal in uplink, we obtain:

$$E_j^k = \sum_{u \in X_b^n} h_{b,u} D_u^k + F_b^k \quad (2)$$

In downlink stage, we rely on the channel tradeoff such as uplink channel evaluate valid estimation for downlink transmission. The BS sends pre-coded downlink channel sequence, such that u 'th user receives downlink the channel signal, $e_{b,u}^{pd}$, given as:

$$e_{b,u}^{pd} = h_{b,u}^T w_{b,u} + F_{b,u}^{pd} \quad (3)$$

where, $w_{b,u} = [w_{b,u}(1) w_{b,u}(2) \dots w_{b,u}(A)]^T = h_{b,u}^*$ is precoding vector for u in b th time slot. This considers that the BS has channel estimation $\mathbb{h}_{b,u}$ before downlink-transmission. We simplify users to set for BS, which has an estimation $h_{b,u}$ as C_b . The single downlink channel symbol is more sufficient; thus rate-loss is neglected. We represent downlink message planned for the user U , $D_u^k = [D_u^k(1) D_u^k(2) \dots D_u^k(M_d)]$ and describe D^d with u th row given by D_u^k for $u \in C_b$. We describe H_b with u th column being $w_{b,u}$ as q th column for $u \in C_b$. The received signal of downlink data is defined as:

$$E_b^d = H_b^T w_b D^d + F_b^k \quad (4)$$

In downlink and uplink, the CT (coherence time) permits T_r symbols and we have $T_r = Z + M = Z + M_k + M_d$. M_k and M_d can be selected as arbitrarily for an asymmetric operation as long as $R = T_r - o$, we undertake the case $M_d = M_k = \frac{M}{2}$. The given data is taken as channel coded with regards to rate \mathcal{R} at the physical level layer, an effective data is $\mathcal{R} \frac{M}{2T_r}$. We also adopt the codes of arbitrary channels with hard identification decoding and put on upper limit on error correcting capabilities for such codes. Specifically, we undertake data/message recovered if $p_e \leq \frac{(1-\mathcal{R})}{2}$, where p_e is defined as the bit-error rate. Henceforth, numerical outcomes serve as UBs from the perspective of channel code. Through C_b , we represent a set of users, whose data-message downlink and uplink are recovered. $C_b \leq Z$ and $|C_b| \leq |X_b|$. In the time slot n , λ_b , system throughput is described as a sum rate.

$$\lambda_b = \frac{|C_b| \mathcal{R} (Z - T_r)}{2T_r} = \frac{|C_b| \mathcal{R} M}{2T_r} \quad (5)$$

Where λ_b is demarcated as recovered data/messages in the time-slot and rate of modulation can be selected as randomly and it will impact the throughput and PD (probability-distribution) $|C_b|$.

2.1. Improvised adaptive channel allocation

In this system, the improvised ACA of communication is defined as downlink and uplink operation. The uplink operation is defined, where communications are organized in successive time-slots as frames. The uplink data is re-sending the data to the improvised ACA methods, if the user is active for more than one time within the frame.

The signals of uplink channels are defined in (1), it is possible to compare and contrast the channels between users and BS. In any case, if more than one user may utilise the same channel sequence, the total of the channels can be evaluated. A superscript \mathcal{H} represents the conjugate transpose and the least squares evaluating $\theta_{j,n}$ is principally based on the channel signal in the j time-slot from the given users are applying c_n is discovered as:

$$\theta_{b,n} = (c_n c_n^{\mathcal{H}})^{-1} E_b^{pk} c_n^{\mathcal{H}} = \sum_{u \in X_b^n} h_{b,u} + f_b^{pk'} \quad (6)$$

where, $f_b^{pk'}$ is processed noise in terms of F_b^{pk} . The vector instance f has prime, which follows the similar definition.

The intrusive users are smearing non-orthogonal and similar channel sequence, which is called channel contamination. In order to identify the information in the uplink stage utilizing an estimation of contaminated channels, summarization of the transmitted data will be one of the outcomes. We represent the estimation of data on channel-estimation $\theta_{b,n}$ by $\varphi_{b,n}$. Considering an orthogonality among the user channels such as $\lim_{A \rightarrow \infty} h_{j,i}^{\mathcal{H}} h_{b,u} / A = 0$ for $a \neq u$.

$$\varphi_{b,n} = (\theta_{b,n}^{\mathcal{H}} \theta_{b,n})^{-1} \theta_{b,n}^{\mathcal{H}} E_b^{pk} = \sum_{u \in X_b^n} \frac{\theta_{b,n}^{\mathcal{H}} h_{b,u}}{\|\theta_{b,n}\|} d_u^k + f_b^{pk'} \quad (7)$$

Anyways, the channel collision leads to the collision of data such as interference between the given data-signals. In order to deal the issue is to reduce the contamination probability by choosing p_x .

The improvised-ACA is represented by a buffer that does not assume the data-collision and the buffers collide the signals and utilize them via an iterative process. We call it improvised-ACA. In order to apply the contaminated as parallel filters on received signals of uplink data, E_b^d , we denote $z_{b,n} \in \mathbb{C}^{1 \times M_k}$.

$$z_{b,n} = \theta_{b,n}^H E_b^{pk} = \sum_{u \in X_b^n} (||h_{b,u}||^2 + \sum_{u \in X_b^n \setminus \{u\}} h_{b,n}^H h_{b,u}) d_u^k + \sum_{v \in X_b \setminus X_b^n} (\sum_{o \in X_b^n} h_{b,o}^H h_{b,v}) d_v^k + f_b^{pk} \quad (8)$$

In contrast to the determination in (6), we do not normalize with channel power estimate. In no-collision mode, the normalization will provide a correct data message. In any case, filtered signals may include several data messages, and channel power may comprise many user channels. After the analogous filtering step and the buffer signals, we arrive at identification.

In order to select an accurate pre-coder for the transmission of downlink, BS may have current channel estimation. The operation of coded is applied in uplink that outcomes in single transmission and more than collisions, it does not ensure that the estimation is available. The operation of uplink relies on the SIC based norm knowledge. Hence, the transmission of downlink to the user, which is possible if the user is to avoid collision during the phase of uplink pilot such that the uncontaminated channel estimation is available. The downlink-transmission reception and considering the channel reciprocity, q th user does not require to evaluate every single $h_{b,u}$, which would need channel signal for A antennas. We receive concatenated channel containing for both downlink precoder W_b and an actual user channel $u, h_{b,u}$. Now, we denoted the concatenated channel $r_{b,u}$, we have:

$$r_{b,u} = h_{b,u}^T W_b \quad (9)$$

where, $r_{b,u}$ is evaluated through (3). The downlink signal part, E_b^d received by the user u is represented as $e_{b,u}^d$. we have:

$$e_{b,u}^d = h_{b,u}^T W_b D^d + f_{b,u}^d = r_{b,u} D^d + f_{b,u}^d \quad (10)$$

Hence, using $r_{b,u}$ estimation, the u th user is capable to recover its own part, d_u^d transmitted message D^d , and it subsequently attempts the decoding at physical-layer.

3. RESULTS AND DISCUSSION

This section describes our experimental setup as well as a performance analysis using cutting-edge methodologies. The system setup, which includes 12 GB RAM and an Intel i5 processor, is compatible with Windows 10. We utilized the MATLAB program to simulate the large MIMO network in the experimental setting. Moreover, the transmission between the BS and the user is established by broadcasting the pilot's signal to compute the channels, which creates channel contamination because the user may interact with the pilots at the same time. In this paper, we present NACAS, which may offer optimum channel allocation while reducing channel contamination in respect of throughput.

With a large weight in an edge-weighted interference graph, the weighted-graph-coloring-based pilot decontamination (WGC-PD) greedily distributes various pilots to linked users. Due to its exponential cumulative feature and resulting computational complexity, WGC-PD in realistic mobile WSN of long-term development technologies may make exhaustive search response to numerous optimization issues untenable. We provide a solution for massive-MIMO channel cognition features based on coded RAS to pilot sequencing. Furthermore, they enable viewing of polluted pilot signals assigned as the graph code, where BP is used to improve the channel approximation procedure.

The number of antennas, transmission power, log-normal shadowing fading, and the number of users is all used to evaluate the performance of our proposed system. Furthermore, for the assessment, comparative approaches such as MRT-ZF [23], WGC-PD [24], and degradation-based pilot scheduling method (DPSM) [25] are utilized with the suggested methodology NACAS. We ran several simulations in which a standard hexagonal cellular network with 10 and 15 cells was used. Each cell contains many users with a single antenna, multiple antennas, and BS, and is surrounded by other cells that are called target cells. The basic parameters considered in our network simulation are shown in Table 1.

Table 2 shows the comparative analysis at number of BS antennas at cell number 10 and 15. Here the throughput has captured at the various number of BS antennas; starts from 10 and goes up to 5000 number of antennas. The throughput is captured on bps/Hz, it varies from 0.138 bps/Hz to 1.695 bps/Hz as per increment of number of antennas in cell 10, while in cell 15; it varies from 0.15 bps/Hz to 1.45 bps/Hz as per increment in number of antennas. More analytical representation has shown in Figures 2-3, where Figure 2 shows the number of BS antennas vs throughput in cell-10. Whereas Figure 3 shows the impact of the number of BS antennas vs throughput in cell-15. At 5000 BS antennas in cell-10, the proposed model NACAS has obtained 8.84%, 12.68%, and 2.71% as compared to WGC-PD, MRT-ZF, and DPSM approach. Similarly considering

cell-15 and 5000 BS antennas, proposed model NACAS has obtained 7.62%, 7.07%, and 3.09% as compared to MRT-ZF, WGC-PD and DPSM approach.

Table 1. Network simulation parameters

Parameters	Values/Range
Number of cells	10, 15
Number of BS antennas	10-5000
Cell radius	500m
Path loss	3.8
Number of users in each cell	10
Spectral efficiency	0.1
The data transmission power	15dB
The pilot transmission power	15dB
Log normal shadowing fading	1-8dB

Table 2. Comparative analysis at number of BS antennas

No. of Antennas	10	50	100	200	500	1000	2000	5000	Method
Cell-10	0.145	0.901	1.139	1.292	1.4	1.352	1.414	1.48	MRT-ZF
	0.149	0.927	1.144	1.324	1.433	1.403	1.435	1.545	WGC-PD
	0.138	0.966	1.175	1.36	1.511	1.528	1.59	1.649	DPSM
	0.166	1.001	1.236	1.392	1.527	1.563	1.602	1.695	NACAS
Cell-15	0.15	1.034	1.07	1.225	1.23	1.238	1.247	1.345	MRT-ZF
	0.154	1.04	1.095	1.263	1.234	1.301	1.268	1.353	WGC-PD
	0.157	1.102	1.113	1.25	1.298	1.328	1.318	1.411	DPSM
	0.161	1.105	1.158	1.332	1.333	1.388	1.39	1.456	NACAS

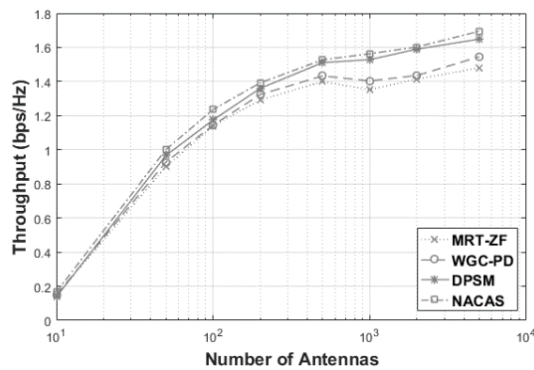


Figure 2. Number of BS antennas vs throughput (cell-10)

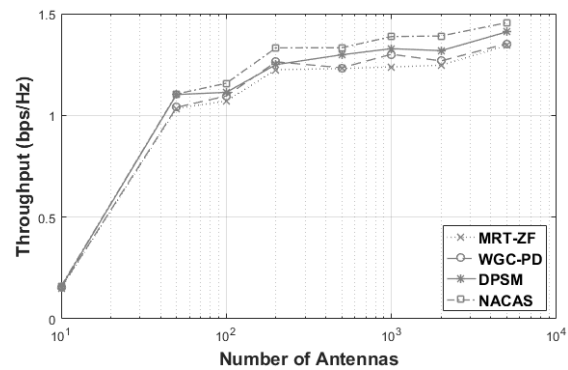


Figure 3. Number of BS antennas vs throughput (cell-15)

In addition, we also considered the shadowing fading effect, where the log normal shadowing fading considered from 1 dB to 8 dB and the complete experimental analysis has shown in Table 3 for cell 10 and cell 15. The throughput is considered to be an evaluation criteria w.r.t log normal fading effect and we found out the proposed model has achieved 4.2%, 6.95%, and -1.05% as compared to WGC-PD, MRT-ZF, and DPSM approach at cell 10 that shown in Figure 4. Similarly in Figure 5 shows log normal shadowing fading vs throughput at cell-15, where proposed model has achieved 6.3%, 8.86%, and 3.66% as compared to WGC-PD, MRT-ZF, and DPSM approach.

Table 3. Comparative analysis at log normal shadowing fading

Fading	1	2	3	4	5	6	7	8	Method
Cell-10	1.434	1.363	1.422	1.462	1.357	1.333	1.472	1.417	MRT-ZF
	1.469	1.335	1.434	1.499	1.381	1.315	1.489	1.459	WGC-PD
	1.532	1.461	1.503	1.517	1.489	1.423	1.561	1.539	DPSM
	1.563	1.485	1.522	1.56	1.499	1.426	1.581	1.523	NACAS
Cell-15	1.265	1.276	1.191	1.222	1.216	1.197	1.281	1.244	MRT-ZF
	1.299	1.304	1.244	1.231	1.222	1.219	1.305	1.279	WGC-PD
	1.329	1.375	1.282	1.295	1.288	1.269	1.353	1.315	DPSM
	1.369	1.396	1.334	1.313	1.309	1.298	1.4	1.365	NACAS

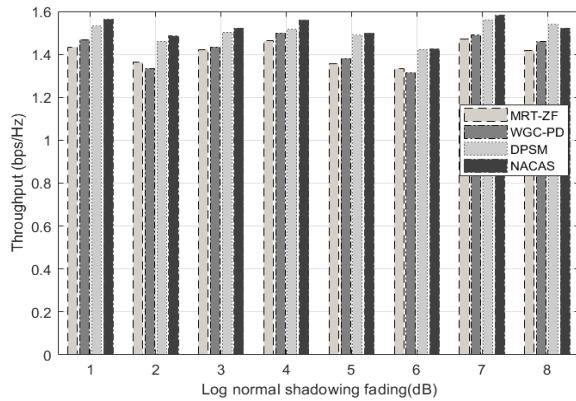


Figure 4. Log normal shadowing fading vs throughput (cell-10)

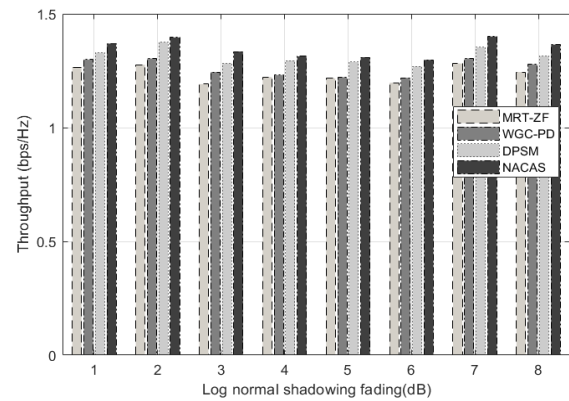


Figure 5. Log normal shadowing fading vs throughput (cell-15)

Table 4 represents the comparative analysis at transmission power at cell 10 and cell 15, where it varies from 2 to 20 and the performance is noted by the achieved throughput. There is lot of variation can be seen at throughput with increasing number of transmission power. At 20 dB transmission power and cell 10, the achievement of NACAS model is 7.29%, 6.53%, and -1.1% as compared to WGC-PD, MRT-ZF, and DPSM approach. The achievement of NACAS model is 5.74%, 4.32%, and -5.74% as compared to WGC-PD, MRT-ZF, and DPSM approach at 20 dB transmission power and cell 15.

Table 4. Comparative analysis at transmission power

Power	2	4	6	8	10	12	14	16	18	20	Method
Cell-10	1.216	1.313	1.283	1.318	1.295	1.544	1.278	1.283	1.37	1.358	MRT-ZF
	1.227	1.31	1.293	1.354	1.336	1.511	1.258	1.279	1.358	1.347	WGC-PD
	1.298	1.352	1.348	1.41	1.362	1.596	1.361	1.366	1.485	1.469	DPSM
	1.296	1.367	1.35	1.456	1.416	1.618	1.377	1.405	1.482	1.453	NACAS
Cell-15	1.159	1.158	1.22	1.12	1.292	1.299	1.315	1.16	1.28	1.349	MRT-ZF
	1.16	1.194	1.233	1.141	1.321	1.297	1.366	1.196	1.358	1.329	WGC-PD
	1.191	1.177	1.25	1.175	1.368	1.36	1.403	1.235	1.334	1.362	DPSM
	1.216	1.226	1.283	1.209	1.436	1.381	1.494	1.285	1.424	1.41	NACAS

The graphical analysis has shown in Figures 6-7 for cell 10 and cell 15. In Figure 8 shows the impact of the number of users on the achievable throughput at cell-10, where proposed model has achieved throughput of 3.28 bps/Hz at 9 number of users. It is very much high as compared to other existing approach. Similarly, Figure 9 shows the impact of the number of users on the achievable throughput at cell-15 where NACAS model is achieved 55%, 62%, and 69% as compared to WGC-PD, MRT-ZF, and DPSM approach at 9 users. The complete numerical analysis for number of user vs throughput has shown in Table 5. The above analysis demonstrates that the proposed NACAS approach can advance the system performance successfully.

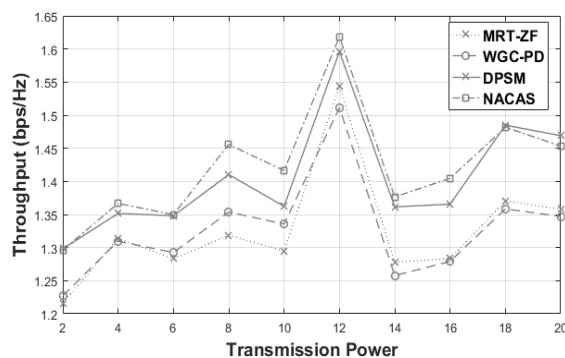


Figure 6. Transmission power vs throughput (cell-10)

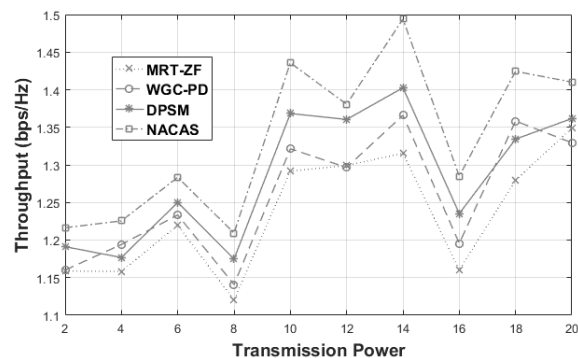


Figure 7. Transmission power vs throughput (cell-15)

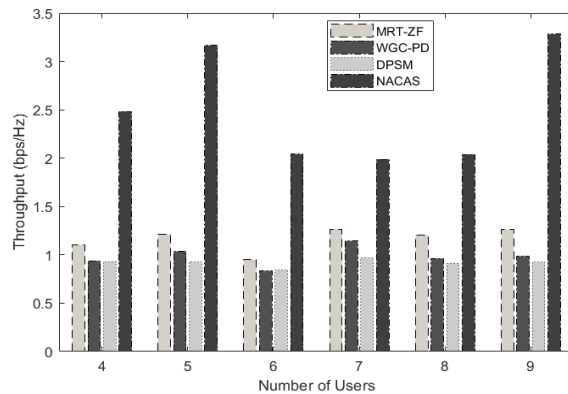


Figure 8. Number of users vs throughput (cell-10)

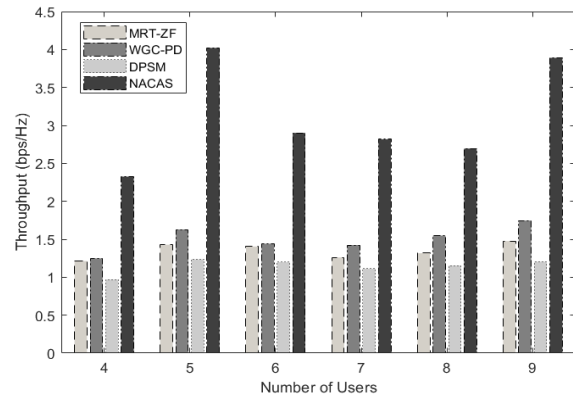


Figure 9. Number of users vs throughput (cell-15)

Table 5. Comparative analysis at number of users

No. of Users	4	5	6	7	8	9	Method
Cell-10	1.106	1.215	0.949	1.266	1.203	1.264	MRT-ZF
	0.938	1.035	0.835	1.144	0.962	0.987	WGC-PD
	0.931	0.927	0.843	0.967	0.912	0.924	DPSM
	2.483	3.166	2.042	1.989	2.039	3.283	NACAS
Cell-15	1.212	1.428	1.404	1.261	1.317	1.477	MRT-ZF
	1.249	1.629	1.441	1.424	1.548	1.746	WGC-PD
	0.97	1.234	1.2	1.112	1.154	1.205	DPSM
	2.326	4.021	2.901	2.817	2.696	3.89	NACAS

4. CONCLUSION

In large MIMO systems, crowd scenarios provide a particularly difficult access challenge. Orthogonal scheduling is impossible due to sporadic user traffic and a lack of pilot sequences. The improvised approach is used to overcome channel problems by optimizing channel allocation. The improvised-ACA is represented by a buffer that does not assume data collision, and the buffers collide and use the signals in an iterative process. The coded operation is used in the uplink, which results in a single transmission, and the uplink operation is based on SIC-based norm knowledge. As a result, downlink transmission to the user avoids collision during the uplink pilot period, allowing for uncontaminated channel estimation. In the result section, we have done several analyses on the proposed NACAS with considering other existing approaches and found out that our proposed scheme has performed well in network validation standards.




REFERENCES

- [1] H. Q. Ngo, A. Ashikhmin, H. Yang, E. G. Larsson, and T. L. Marzetta, "Cell-Free Massive MIMO: Uniformly great service for everyone," *2015 IEEE 16th International Workshop on Signal Processing Advances in Wireless Communications (SPAWC)*, 2015, pp. 201–205, doi: 10.1109/SPAWC.2015.7227028.
- [2] H. Q. Ngo, A. Ashikhmin, H. Yang, E. G. Larsson, and T. L. Marzetta, "Cell-Free Massive MIMO Versus Small Cells," *IEEE Trans. On Wireless Commun.*, 2017, vol. 16, no. 3, pp. 1834–1850, doi: 10.1109/TWC.2017.2655515.
- [3] S. Elhoushy and W. Hamouda, "Performance of Distributed Massive MIMO and Small-Cell Systems Under Hardware and Channel Impairments," in *IEEE Transactions on Vehicular Technology*, vol. 69, no. 8, pp. 8627–8642, Aug. 2020, doi: 10.1109/TVT.2020.2998405.
- [4] H. Q. Ngo, A. Ashikhmin, H. Yang, E. G. Larsson and T. L. Marzetta, "Correction to "Cell-Free Massive MIMO Versus Small Cells" [Mar 17 1834–1850]," in *IEEE Transactions on Wireless Communications*, vol. 19, no. 5, pp. 3623–3624, May 2020, doi: 10.1109/TWC.2020.2974209.
- [5] N. Akbar, E. Björnson, N. Yang, and E. G. Larsson, "Max-Min Power Control in Downlink Massive MIMO With Distributed Antenna Arrays," *IEEE Transactions on Communications*, vol. 69, no. 2, pp. 740–751, Feb. 2021, doi: 10.1109/TCOMM.2020.3033018.
- [6] C. Lv, J. -C. Lin, and Z. Yang, "CSI Calibration for Precoding in mmWave Massive MIMO Downlink Transmission Using Sparse Channel Prediction," *IEEE Access*, vol. 8, pp. 154382–154389, 2020, doi: 10.1109/ACCESS.2020.3017787.
- [7] D. Sarkar, Y. Antar, and S. Mikki, "Controlling Microwave and Millimeter Wave Massive MIMO Uplink Channel Capacity Using Reconfigurable FSS Structures," *2019 IEEE MTT-S International Microwave and RF Conference (IMARC)*, 2019, pp. 1–4, doi: 10.1109/IMaRC45935.2019.9118754.
- [8] S. Ghosh and R. Chopra, "Downlink Pilots for Hybrid Massive MIMO Under Reciprocity Imperfections," *IEEE Communications Letters*, vol. 24, no. 10, pp. 2334–2338, Oct. 2020, doi: 10.1109/LCOMM.2020.3004001.
- [9] J. W. Ma, D. Liu, Y. Liu, W. Pan, and H. Zhao, "On the Capacity of ZF Beamforming in Massive MIMO Systems with Imperfect Reciprocity Calibration," *2017 IEEE Globecom Workshops (GC Wkshps)*, 2017, pp. 1–5, doi: 10.1109/GLOCOMW.2017.8269165.




- [10] C. Chen *et al.*, "Distributed Massive MIMO: A Diversity Combining Method for TDD Reciprocity Calibration," *GLOBECOM 2017 - 2017 IEEE Global Communications Conference*, 2017, pp. 1-7, doi: 10.1109/GLOCOM.2017.8254817.
- [11] V. Kumar, S. K. Patra, and P. Singh, "Mean-based reciprocity calibration in TDD massive MIMO system," *IET Communications*, vol. 14, no. 22, pp. 4038 – 4047, 27 December 2020, doi: 10.1049/iet-com.2019.1049.
- [12] S. A. Khwandah, J. P. Cosmas, P. I. Lazaridis, Z. D. Zaharis, and I. P. Chochliouros, "Massive MIMO Systems for 5G Communications," *Wireless Personal Communications*, vol. 120, pp. 2101–2115, 2021, doi: 10.1007/s11277-021-08550-9.
- [13] E. Bjornson, J. Hoydis, M. Kountouris, and M. Debbah, "Massive MIMO Systems with Non-Ideal Hardware: Energy Efficiency, Estimation, And Capacity Limits," in *IEEE Transactions on Information Theory*, vol. 60, no. 11, pp. 7112–7139, Nov. 2014, doi: 10.1109/TIT.2014.2354403.
- [14] D. Inserra and A. M. Tonello, "Characterization of Hardware Impairments in Multiple Antenna Systems For Doa Estimation," *Journal of Electrical and Computer Engineering*, vol. 2011, no. 1, pp. 1–10, Dec. 2011, doi: 10.1155/2011/908234.
- [15] J. M. Palacios, O. Raeesi, A. Gokceoglu, and M. Valkama, "Impact of Channel Non-Reciprocity in Cell-Free Massive MIMO," in *IEEE Wireless Communications Letters*, vol. 9, no. 3, pp. 344–348, March 2020, doi: 10.1109/LWC.2019.2954513.
- [16] D. Mi, M. Dianati, L. Zhang, S. Muhaidat, and R. Tafazolli, "Massive MIMO Performance With Imperfect Channel Reciprocity and Channel Estimation Error," in *IEEE Transactions on Communications*, vol. 65, no. 9, pp. 3734–3749, Sept. 2017, doi: 10.1109/TCOMM.2017.2676088.
- [17] J. Choi, D. J. Love, and P. Bidigare, "Downlink Training Techniques for FDD Massive MIMO Systems: Open-Loop and Closed-Loop Training With memory," *IEEE Journal of Selected Topics in Signal Processing*, vol. 8, no. 5, pp. 802–814, Oct. 2014, doi: 10.1109/JSTSP.2014.2313020.
- [18] S. Bazzi and W. Xu, "Downlink Training Sequence Design for FDD Multiuser Massive MIMO Systems," *IEEE Transactions on Signal Processing*, vol. 65, no. 18, pp. 4732–4744, Sep. 2017, doi: 10.1109/TSP.2017.2711522.
- [19] T. E. Bogale, L. B. Le, A. Haghighat, and L. Vandendorpe, "On the Number of RF Chains And Phase Shifters, and Scheduling Design With Hybrid Analog-Digital Beamforming," *IEEE Transactions on Wireless Communications*, vol. 15, no. 5, pp. 3311–3326, May 2016, doi: 10.1109/TWC.2016.2519883.
- [20] T. L. Marzetta, "Massive MIMO: An Introduction," *Bell Labs Technical Journal*, vol. 20, pp. 11–22, 2015, doi: 10.15325/BLTJ.2015.2407793.
- [21] O. Elijah, C. Y. Leow, T. A. Rahman, S. Nunoo, and S. Z. Iliya, "A Comprehensive Survey of Pilot Contamination in Massive MIMO—5G System," in *IEEE Communications Surveys & Tutorials*, vol. 18, no. 2, pp. 905–923, 2016, doi: 10.1109/COMST.2015.2504379.
- [22] X. Nie and F. Zhao, "Pilot Allocation and Power Optimization of Massive MIMO Cellular Networks With Underlaid D2D Communications," in *IEEE Internet of Things Journal*, vol. 8, no. 20, pp. 15317–15333, 2021, doi: 10.1109/JIOT.2021.3061510.
- [23] J. Li, D. Wang, P. Zhu, J. Wang, and X. You, "Downlink Spectral Efficiency of Distributed Massive MIMO Systems With Linear Beamforming Under Pilot Contamination," in *IEEE Transactions on Vehicular Technology*, vol. 67, no. 2, pp. 1130–1145, Feb. 2018, doi: 10.1109/TVT.2017.2733532.
- [24] X. Zhu, L. Dai, Z. Wang, and X. Wang, "Weighted-Graph-Coloring-Based Pilot Decontamination for Multicell Massive MIMO Systems," in *IEEE Transactions on Vehicular Technology*, vol. 66, no. 3, pp. 2829–2834, March 2017, doi: 10.1109/TVT.2016.2572203.
- [25] Y. Wu, T. Liu, M. Cao, L. Li, and W. Xu, "Pilot contamination reduction in massive MIMO systems based on pilot scheduling," *EURASIP Journal on Wireless Communications and Networking*, vol. 1, pp. 1–9, 2018, doi: 10.1186/s13638-018-1029-1.

BIOGRAPHIES OF AUTHORS



Sandeep Dhanraj Bawage    completed B.E (Electronics and Communication Engineering), M.Tech (Communication System) and perusing Ph.D from VTU, Belagavi, India. Research work at performance analysis of Wimax based OFDM system. The area of interest in wireless communication, digital processing. Member of ISTE, IETE. He can be contacted at email: sandeepbawage@gmail.com.



Manjula Shivkumar    received the B.E in Electronics and Communication Engineering from Gulbarga University in 1997 and M.Tech in Electronics and Communication Engineering from RVD University in 2006 and Ph.D degree from Singhania University in 2014. She became an Assistant professor in 1998, an Associate professor in 2007 and Professor of E & CE dept in 2014. She has authored or coauthored more than 20 referred journal and conference papers. Her research interest includes Synthesis characterization and microwave properties of conducting polymer composites. Member of ISTE, IETE. She can be contacted at email: manjulasidramshetty@gmail.com.